Materials Letters 211 (2018) 87–90

Contents lists available at ScienceDirect

Materials Letters

journal homepage: www.elsevier.com/locate/mlblue

Aging behavior of the HfNbTaTiZr high entropy alloy

N.D. Stepanov [a,*], N.Yu. Yurchenko [a], S.V. Zherebtsov [a], M.A. Tikhonovsky [b], G.A. Salishchev [a]

[a] Laboratory of Bulk Nanostructured Materials, Belgorod State University, Belgorod 308015, Russia
[b] National Science Center "Kharkov Institute of Physics and Technology" NAS of Ukraine, Kharkov 61108, Ukraine

ARTICLE INFO

Article history:
Received 25 July 2017
Received in revised form 6 September 2017
Accepted 25 September 2017
Available online 27 September 2017

Keywords:
Metals and alloys
High entropy alloys
Phase transformation
Heat treatment
TEM

ABSTRACT

The HfNbTaTiZr high entropy alloy was produced by vacuum arc melting, homogenized at 1200 °C, and annealed at 600–1000 °C for 1–100 h. Structure and microhardness of the annealed alloy were investigated. A strong increase of microhardness after aging treatment at 600 °C was found. Formation of second hcp phase particles in the bcc matrix after annealing at 600 and 800 °C was also revealed. Effect of precipitation of second phase particles on microhardness was analyzed.

1. Introduction

High entropy alloys (HEAs) are generally defined as multicomponent (≥5 elements) nearly equiatomic (the concentration of the principle components is 5–35 at.%) metallic alloys [1–3]. The initial idea behind this concept was that high entropy of mixing natural for the multicomponent equiatomic alloys can make the formation of solid solution phases more preferable over intermetallic ones [1]. Several HEAs with single solid solution phase structures have been found so far. The best-known example is the equiatomic CoCrFeNiMn alloy with a single face-centered cubic (fcc) structure introduced by Cantor [4–7]. Several body-centered cubic (bcc) structured HEAs were also introduced [8,9]. These bcc HEAs are mostly based on refractory elements, and the best-studied example among them is the HfNbTaTiZr alloy [10–13].

Although the initial HEA concept emphasized formation of a single solid solution phase, the strength of many commercial structural metallic materials increases usually by second phases in order to meet the required characteristics [14]. However approaches to precipitates formation in a disordered matrix in refractory elements based HEAs in a controlled way are still unclear. For instance, it is already established by O.N. Senkov et al. that the HfNbTaTiZr alloy (i) has the single bcc phase after homogenization treatment [10]; (ii) second phase particles can be found in the alloy after deformation at elevated temperatures or annealing [11,13]. But the possibility of hardening heat treatment of the alloy has not been revealed yet. Therefore, in this work we have studied an annealing effect on the hardness and structure of the homogenized equiatomic HfNbTaTiZr alloy.

2. Materials and methods

The equiatomic HfNbTaTiZr alloy was produced by vacuum arc melting. Pure elements (each of them at least 99.9% purity) were used as the raw material. The ingot with dimensions $\approx 8 \times 12 \times 40$ mm^3 was remelted 5 times to ensure the chemical homogeneity. The obtained alloy had an equiatomic composition (20 ± 1 at.% of each component). The as-cast alloy was homogenized in vacuum at 1200 °C for 24 h. After homogenization, the alloy was annealed in vacuum at 600, 800 and 1000 °C for 1–100 h. The microhardness of the alloy was measured with 200 g load. Each data point was the average of at least 20 individual measurements. The structure was characterized by X-ray diffraction (XRD), scanning (SEM) and transmission (TEM) electron microscopy. The XRD measurements were performed using a Riguku diffractometer with Cu radiation. A Quanta 200 3D microscope with energy dispersive (EDX) detector was used for the SEM analysis. TEM images were obtained using a JEOL JEM-2100 microscope equipped with EDX detector. Samples for the TEM investigation were prepared by twin-jet electropolishing in a mixture of 5 mL HF + 45 mL H2SO4 in 950 methanol at −35 °C.

* Corresponding author.
E-mail addresses: stepanov@bsu.edu.ru, stepanov.nikita@icloud.com (N.D. Stepanov).

https://doi.org/10.1016/j.matlet.2017.09.094

3. Results and discussion

In the initial homogenized condition the HfNbTaTiZr alloy had a single phase bcc structure (Fig. 1a). The lattice parameter of the bcc phase was 0.340 nm. SEM-BSE image (Fig. 1b) shows the presence of coarse grains with the mean size of 185 ± 75 μm.

Fig. 2 shows the microhardness of the HfNbTaTiZr alloy depending on the annealing conditions (temperature and time). The hardness of the alloy in the homogenized condition was 370 HV. Annealing for 1 h at 800 °C and 1000 °C resulted in slight (≈10%) increase of the microhardness. Further annealing for 10 and 100 h at these temperatures caused a decrease of hardness approximately to the initial level. The hardness was somewhat higher after annealing at 800 °C for all soak time. Annealing at 600 °C had much more pronounced effect: after 1-h annealing the microhardness rose to 470 HV. An increase in annealing time to 10 h resulted in further increase of the microhardness to 500 HV, i.e. an increment in hardness by ≈35% in comparison with the initial condition was achieved. Further increase of annealing time resulted in gradual softening. Nevertheless, the microhardness of the alloy annealed at 600 °C for 15–100 h was still significantly higher than that in the initial condition (450–465 HV vs. 370 HV, Fig. 2).

To understand the reasons of hardening of the HfNbTaTiZr alloy after annealing, microstructural studies were performed. The SEM investigation of the HfNbTaTiZr alloy after 10-h annealing at 600 °C had revealed some second phase particles in grain boundaries; however more detailed TEM study (Fig. 3a) had shown numerous

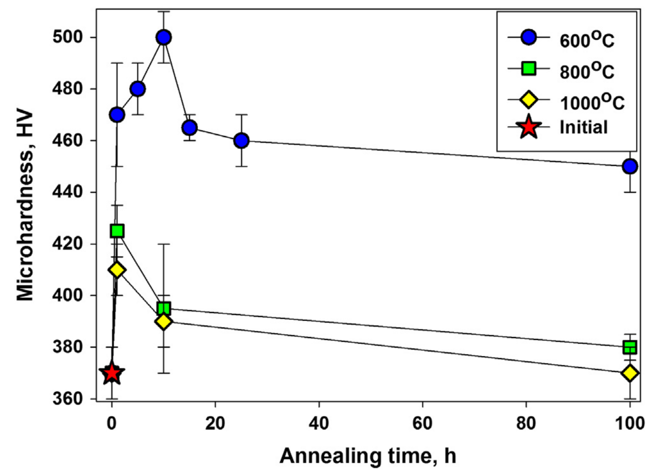

Fig. 2. The dependence of microhardness of the HfNbTaTiZr alloy on annealing temperature and time.

nano-sized particles with a hexagonal close-packed (hcp) lattice (a = 0.297 nm; c = 0.478 nm). Their volume fraction was ~20% and the average diameter was 25 nm. The particles were enriched with Hf and Ta (≈25 at.% each). The grain boundary particles were much coarser (several hundred nm), but had the same crystal structure and chemical composition. Further increase of the soak time at 600 °C to 100 h resulted in the complete decomposition of the initial single phase structure and the formation of a fine basket-weave-like structure (Fig. 3b). According to the XRD results (Fig. 1a), the structure was composed of the bcc and hcp phases. Note that the lattice parameter of the bcc phase decreased in comparison with the initial condition, possibly due to changes in the chemical composition. At a higher temperature (800 °C), the second phase particles with the average size of several microns appeared after 10 and 100 h annealing (Fig. 3c and d respectively). The particles were mainly found in (sub)grain boundaries in a form of characteristic chains inside bcc grains. Some individual particles were also observed however. The volume fraction of the particles increased from 12% to 21% with an increase of annealing time from 10 to 100 h. The particles were enriched with Hf and Ta and in accordance with the XRD results (Fig. 1a) had the hcp structure. Note that the previous studies have reported the formation of the second phase with bcc structure in the HfNbTaTiZr alloy after annealing at 800 °C [11,15]. However, the experimental conditions like initial state (homogenized vs cold-rolled) and annealing time (10–100 h vs 2 h) in present and previous works were different. This is probably the reason for the discrepancy between the obtained results. The investigations of the HfNbTaTiZr alloy after annealing at 1000 °C (not shown) had revealed predominantly a single-phase structure similar to that observed in the homogenized condition, however with a tiny fraction of unidentified second phase particles in grain boundaries.

The presence of nano-sized second (hcp) phase particles in the HfNbTaTiZr alloy after annealing (aging) at 600 °C for 10 h (Fig.3a) most likely resulted in the pronounced increase in hardness (Fig. 2). The hardening effect of the precipitates can be estimated using the Ashby-Orowan equation [16]:

$$\Delta\sigma = 0.538Gb\left(\frac{\sqrt{f}}{d}\right)ln\left(\frac{d}{2b}\right) \quad (1)$$

where G is the shear modulus, b is the Burgers vector, f is the volume fraction of particles, and d is their diameter. The f and d values were given above. The shear modulus of ≈100 GPa for the HfNbTaTiZr alloy at room temperature was reported in [11], the Burgers

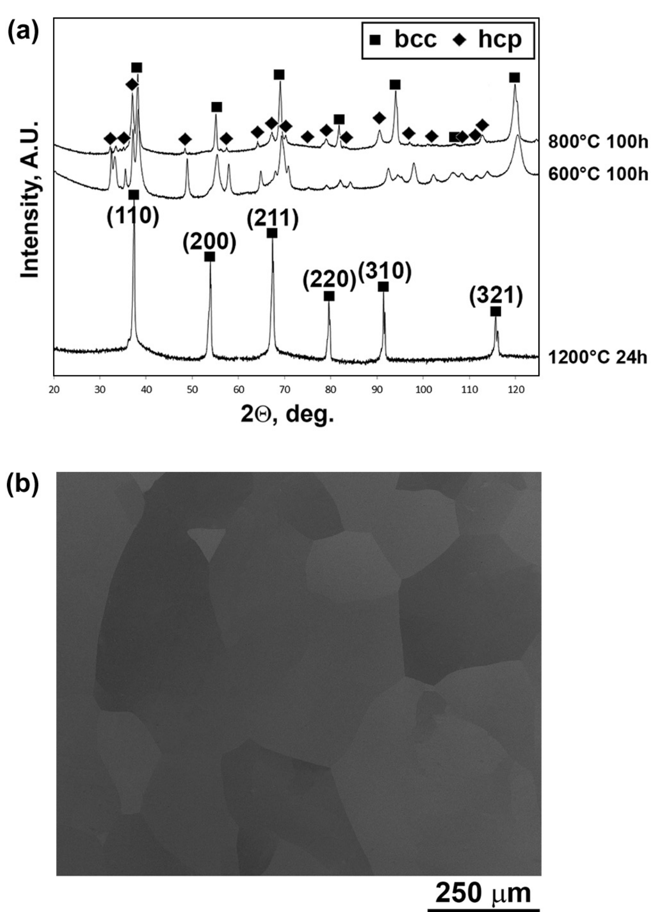

Fig. 1. Structure of the HfNbTaTiZr alloy: XRD patterns of the alloy in the homogenized and annealed (600 °C, 100 h, and 800 °C, 100 h) conditions (a) and SEM-BSE image of the alloy in the homogenized condition (b).

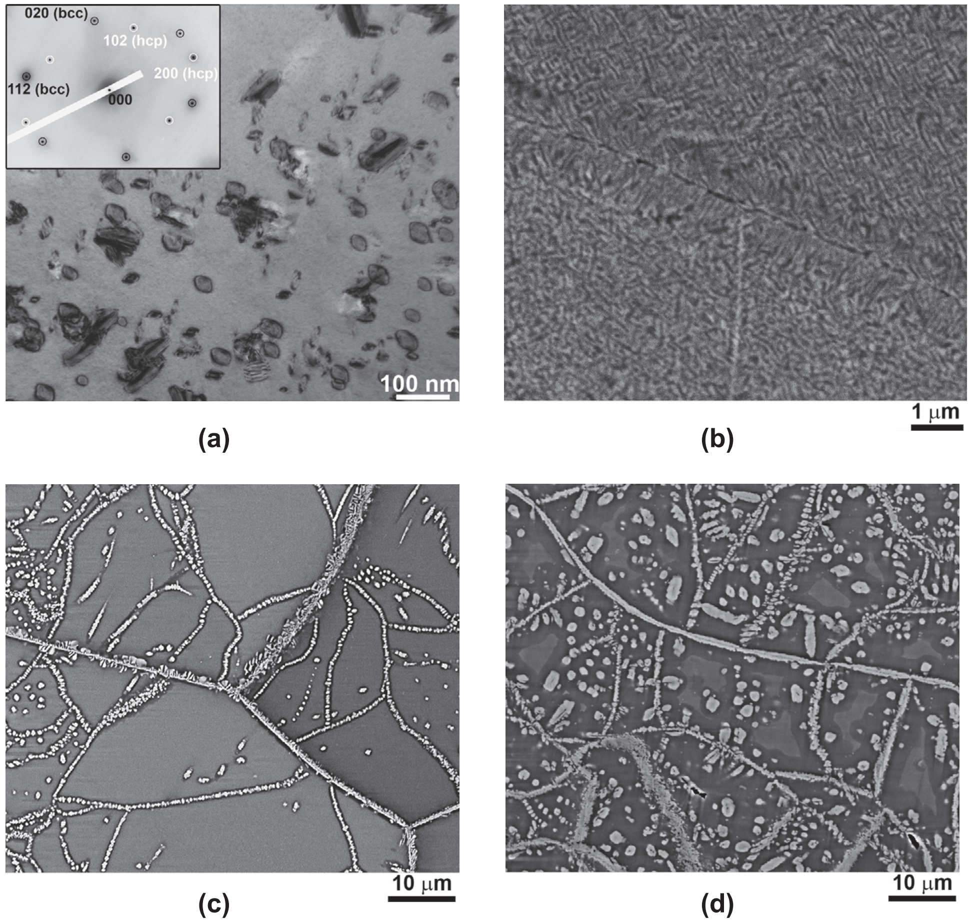

Fig. 3. Microstructure of the HfNbTaTiZr alloy after annealing at 600 °C (a, b), 800 °C (c, d) for 10 (a, c) and 100 (b, d) hours.

vector can be estimated as of 0.245 nm using the experimental bcc lattice parameter. Converting the results of Eq. (1) to microhardness HV, we had obtained the microhardness increase $\Delta HV \approx 110$. This value is consistent with the experimental increase in the microhardness by 130 HV (Fig. 3) and proves that the precipitation of the nanoscale hcp particles after 10 h annealing at 600 °C can cause a significant increase of hardness. It seems reasonable to suggest that the coarsening of the second phase particles due to longer annealing (Fig. 3b) resulted in a diminishing of strengthening effect in accordance with Eq. (1). Similarly, the micron-sized hcp particles produced by annealing at 800 °C (Fig. 3c and d) did not cause significant strengthening (Fig. 2).

In general, the obtained data demonstrate that a significant strengthening of the HfNbTaTiZr alloy can be achieved by an aging treatment due to the precipitation of the nano-sized second phase particles. This is an important result since both the work hardening [11] and grain refinement [17] have a weak effect on strength of the alloy. For instance, microhardness of the alloy after cold rolling with 86.4% thickness reduction is 366 HV [11] (compare with 500 HV after annealing at 600 °C). It should be also noted that in the CoCrFeNiMn alloy precipitation of second phases did not result in a pronounced hardening [18,19]. On the other hand, the microstructural observations demonstrated that the high-temperature single phase structure of the alloy (Fig. 1) became drastically unstable at lower temperatures (i.e. Fig. 3b). This might limit the potential application of the HfNbTaTiZr alloy as a high-temperature material. Possibly, the chemical composition of the alloy could be modified to improve both the structural stability and hardening response; however this is the task for further investigations.

4. Conclusions

The effect of annealing at 600–1000 °C for 1–100 h on the structure and microhardness of the homogenized (1200 °C, 24 h) HfNbTaTiZr alloy was investigated. It was revealed that the microhardness increased from 370 HV in the homogenized condition to 500 HV after aging at 600 °C for 10 h. The hardening was associated with the precipitation of the Hf, Ta-rich hcp particles in the bcc matrix of the alloy. The formation of the second hcp phase was also observed after annealing at 800 °C; however the hardening effect was noticeably lower due to the larger size of the particles. At both temperatures, the fraction of hcp phase increased with the increase of soak time.

Acknowledgments

The authors gratefully acknowledge the financial support from Russian Science Foundation, Grant № 14-19-01104. The authors are also grateful to Joint Research Center "Materials and Technologies", Belgorod State University, for the assistance with instrumental analysis.

References

[1] J.-W. Yeh, S.-K. Chen, S.-J. Lin, J.-Y. Gan, T.-S. Chin, T.-T. Shun, C.-H. Tsau, S.-Y. Chang, Nanostructured high-entropy alloys with multiple principal elements: novel alloy design concepts and outcomes, Adv. Eng. Mater. 6 (2004) 299–303, https://doi.org/10.1002/adem.200300567.
[2] Y. Zhang, T.T. Zuo, Z. Tang, M.C. Gao, K.A. Dahmen, P.K. Liaw, Z.P. Lu, Microstructures and properties of high-entropy alloys, Prog. Mater. Sci. 61 (2014), https://doi.org/10.1016/j.pmatsci.2013.10.001.

[3] D.B. Miracle, O.N. Senkov, A critical review of high entropy alloys and related concepts, Acta Mater. 122 (2017) 448–511, https://doi.org/10.1016/j.actamat.2016.08.081.
[4] B. Cantor, I.T.H. Chang, P. Knight, A.J.B. Vincent, Microstructural development in equiatomic multicomponent alloys, Mater. Sci. Eng. A 375 (2004) 213–218, https://doi.org/10.1016/j.msea.2003.10.257.
[5] F. Otto, Y. Yang, H. Bei, E.P.P. George, Relative effects of enthalpy and entropy on the phase stability of equiatomic high-entropy alloys, Acta Mater. 61 (2013) 2628–2638, https://doi.org/10.1016/j.actamat.2013.01.042.
[6] G.A. Salishchev, M.A. Tikhonovsky, D.G. Shaysultanov, N.D. Stepanov, A.V. Kuznetsov, I.V. Kolodiy, A.S. Tortika, O.N. Senkov, Effect of Mn and V on structure and mechanical properties of high-entropy alloys based on CoCrFeNi system, J. Alloys Compd. 591 (2014) 11–21, https://doi.org/10.1016/j.jallcom.2013.12.210.
[7] M. Laurent-Brocq, A. Akhatova, L. Perrière, S. Chebini, X. Sauvage, E. Leroy, Y. Champion, Insights into the phase diagram of the CrMnFeCoNi high entropy alloy, Acta Mater. 88 (2015), https://doi.org/10.1016/j.actamat.2015.01.068.
[8] O.N. Senkov, G.B. Wilks, D.B. Miracle, C.P. Chuang, P.K. Liaw, Refractory high-entropy alloys, Intermetallics 18 (2010) 1758–1765, https://doi.org/10.1016/j.intermet.2010.05.014.
[9] O.N. Senkov, G.B. Wilks, J.M. Scott, D.B. Miracle, Mechanical properties of Nb25Mo25Ta25W25 and V20Nb20Mo20Ta20W20 refractory high entropy alloys, Intermetallics 19 (2011) 698–706, https://doi.org/10.1016/j.intermet.2011.01.004.
[10] O.N. Senkov, J.M. Scott, S.V. Senkova, D.B. Miracle, C.F. Woodward, Microstructure and room temperature properties of a high-entropy TaNbHfZrTi alloy, J. Alloys Compd. 509 (2011) 6043–6048, https://doi.org/10.1016/j.jallcom.2011.02.171.
[11] O.N. Senkov, S.L. Semiatin, Microstructure and properties of a refractory high-entropy alloy after cold working, J. Alloys Compd. 649 (2015) 1110–1123, https://doi.org/10.1016/j.jallcom.2015.07.209.
[12] J.-P. Couzinié, L. Lilensten, Y. Champion, G. Dirras, L. Perrière, I. Guillot, On the room temperature deformation mechanisms of a TiZrHfNbTa refractory high-entropy alloy, Mater. Sci. Eng. A 645 (2015) 255–263, https://doi.org/10.1016/j.msea.2015.08.024.
[13] O.N. Senkov, J.M. Scott, S.V. Senkova, F. Meisenkothen, D.B. Miracle, C.F. Woodward, Microstructure and elevated temperature properties of a refractory TaNbHfZrTi alloy, J. Mater. Sci. 47 (2012) 4062–4074, https://doi.org/10.1007/s10853-012-6260-2.
[14] D.B. Miracle, Critical Assessment 14: High entropy alloys and their development as structural materials, Mater. Sci. Technol. 31 (2015) 1142–1147, https://doi.org/10.1179/1743284714Y.0000000749.
[15] W. Wu, S. Ni, Y. Liu, M. Song, Effects of cold rolling and subsequent annealing on the microstructure of a HfNbTaTiZr high-entropy alloy, J. Mater. Res. 31 (2016) 3815–3823, https://doi.org/10.1557/jmr.2016.445.
[16] T. Gladman, Precipitation hardening in metals, Mater. Sci. Technol. 15 (1999) 30–36, https://doi.org/10.1179/026708399773002782.
[17] C.-C.C. Juan, M.-H.H. Tsai, C.-W.W. Tsai, W.-L.L. Hsu, C.-M.M. Lin, S.-K.K. Chen, S.-J.J. Lin, J.-W.W. Yeh, Simultaneously increasing the strength and ductility of a refractory high-entropy alloy via grain refining, Mater. Lett. 184 (2016) 200–203, https://doi.org/10.1016/j.matlet.2016.08.060.
[18] B. Schuh, F. Mendez-Martin, B. Völker, E.P.P. George, H. Clemens, R. Pippan, A. Hohenwarter, B. Volker, E.P.P. George, H. Clemens, R. Pippan, A. Hohenwarter, Mechanical properties, microstructure and thermal stability of a nanocrystalline CoCrFeMnNi high-entropy alloy after severe plastic deformation, Acta Mater. 96 (2015) 258–268, https://doi.org/10.1016/j.actamat.2015.06.025.
[19] N.D.D. Stepanov, D.G.G. Shaysultanov, M.S.S. Ozerov, S.V.V. Zherebtsov, G.A.A. Salishchev, Second phase formation in the CoCrFeNiMn high entropy alloy after recrystallization annealing, Mater. Lett. 185 (2016) 1–4, https://doi.org/10.1016/j.matlet.2016.08.088.